Cell, Vol. 61, 579–589, May 18, 1990, Copyright © 1990 by Cell Press

Mutations of Phosphorylation Sites in Lamin A That Prevent Nuclear Lamina Disassembly in Mitosis

Rebecca Heald and Frank McKeon
Department of Cellular and Molecular Physiology
Harvard Medical School
Boston, Massachusetts 02115

Summary

The nuclear envelope is a dynamic structure that completely disassembles in response to MPF/*cdc2* activity in mitosis. A key feature of this process is the hyperphosphorylation of the major structural proteins of the envelope, the nuclear lamins A, B, and C. Two highly conserved serine residues of the lamin protein (Ser-22 and Ser-392 of lamins A and C) are symmetrically positioned 5 amino acids from the ends of the large α-helical domain and are shown in the accompanying paper by Ward and Kirschner to be among four sites phosphorylated during nuclear envelope breakdown. Mutations in Ser-22 and Ser-392 that prevent phosphorylation at these sites block the disassembly of the nuclear lamina during mitosis. We propose a model for the regulation of lamin assembly in which phosphorylation just outside the ends of the α-helical domain controls the assembly dynamics of the lamin coiled-coil dimers.

Introduction

The assembly and disassembly of the nuclear lamins during the cell cycle are conserved features of higher eukaryotes. The nuclear lamin proteins (A, B, and C) interact to form a supramolecular complex on the inner surface of the nuclear membranes (Newport and Forbes, 1987; Gerace and Burke, 1988). Changes in nuclear architecture and incorporation of newly synthesized lamins into the nuclear envelope during interphase imply a dynamic state of lamin interactions. A more significant change in lamin association occurs during mitosis, when the activation of MPF/*cdc2* induces a phosphorylation cascade coincident with lamina disassembly (Maller et al., 1977; Miake-Lye and Kirschner, 1985). The disassembled mitotic lamins have been shown to be hyperphosphorylated and appear to be dephosphorylated upon reassembly around daughter nuclei (Gerace and Blobel, 1980; Burke and Gerace, 1986).

Knowledge of the structure of the nuclear lamin proteins, their modes of assembly, and their sites of phosphorylation is necessary to understand how mitotic signals regulate so dramatically the structure of the nucleus. Clues for understanding the structural basis of nuclear lamin assembly came from the cloning of the lamin cDNAs. The predicted amino acid sequences of the lamin proteins revealed strong primary and secondary structural homologies with the α helices of a well-studied class of proteins, the cytoplasmic intermediate filaments (McKeon et al., 1986; Fisher et al., 1986). The cytoplasmic intermediate filament proteins form coiled-coil dimers, which subsequently assemble into higher order, 10 nm filaments based on dimer–dimer interactions. These proteins exhibit variable states of assembly in mitosis (Crick, 1953; Parry et al., 1987; Hynes and Destree, 1978; Franke et al., 1978; Chou et al., 1989). The lamin proteins not only share evolutionary origins with the intermediate filament class of proteins, but also possess a dimer subunit that assembles into 10 nm filaments and paracrystalline arrays in vitro. They appear as 10 nm, orthogonally arranged filaments at the nuclear envelope (Aebi et al., 1986; Parry et al., 1987; Ward and Kirschner 1990).

Not clear from the structural models is how an MPF/*cdc2*-induced phosphorylation cascade causes the catastrophic disassembly of the higher order lamin structure during mitosis. A surprising observation was that the overall increase in lamin phosphorylation during the mitotic transition is small, equivalent to an average of two additional phosphates per molecule (Ottaviano and Gerace, 1985). One explanation that could account for this low stoichiometry is that the MPF-induced lamin phosphorylation affects highly sensitive domains in the lamin proteins required for assembly. In lieu of any sequence information on the lamin phosphorylation sites, we initially approached this problem purely from structural considerations; these were supported by the direct sequencing of phosphorylation sites on lamin C by Ward and Kirschner (1990). Both the structural and sequence considerations focused on Ser-22 and Ser-392 as key sites that might be involved in the regulation of lamin assembly and disassembly during the cell cycle. We proceeded by introducing changes at Ser-22 and Ser-392 in the human lamin A cDNA and expressing the proteins in Chinese hamster ovary (CHO) cells. While changes at Ser-392 yield a wild-type mitotic phenotype in transfected cells, mutations at Ser-22 result in unusual mitotic phenotypes in which 35% of the mitotic cells retain the nuclear lamina. Double mutations at Ser-22 and Ser-392 block the disassembly of the lamina in an overwhelming majority of the mitotic cells. In addition, we show that point mutations in the highly conserved end domains of the α helix, but not in the central α-helical domains of the molecule, abolish the protein's assembly potential. These structural alterations in the end domains that prevent assembly may simulate the perturbations induced by phosphorylation of the nearby Ser-22 and Ser-392 residues.

Results

Symmetry of Conserved Serines Adjacent to the α Helix

Phosphoamino acid analysis of the nuclear lamin proteins indicated that the phosphorylation sites were predominately serine residues (Dessev et al., 1988). To determine the likely target serine residues, we compared the amino acid sequences of lamins A, B, and C from human, mouse, and frog origins and found 14 highly conserved serine

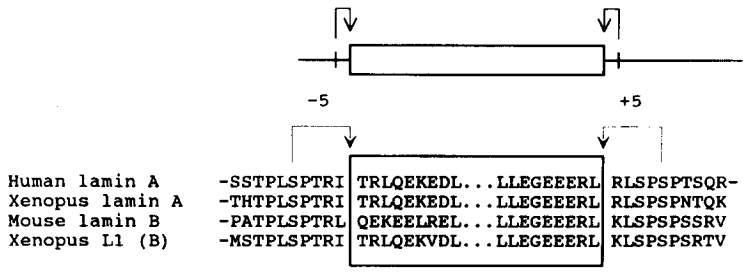

Figure 1. Symmetry of Conserved Serines about the α Helix

Ser-22 and Ser-392 of the human lamin A and C proteins are 2 of 14 serine residues conserved in the lamin proteins from human to Xenopus laevis. Their positions display symmetry about the ends of the large (360 amino acids, shown boxed) α helix as defined by limits of the region conserved in intermediate filaments (Geisler and Weber, 1982; McKeon et al., 1986). Ser-22 and Ser-392 and their homologs in the mouse and Xenopus lamins can be accommodated within the general sequence S/TP#SPT/S (# = single or no residue).

residues (McKeon et al., 1986; Fisher et al., 1986; Krohne et al., 1987; Wolin et al., 1987; Hoger et al., 1988). One of these conserved serine residues falls in the non-α-helical N-terminus, four within the large α helix itself, and the remaining nine within the non-α-helical C-terminus. Two of these serine residues stand out because they are surrounded by blocks of amino acids with homology to one another—Ser-22 within TPLS^{22}PT and Ser-392 within LSPS^{392}PT—and because they are symmetrically arranged about the conserved domains of the α helix (Figure 1). Ser-22 lies exactly 5 residues before the beginning of the conserved α-helical domain found in all intermediate filaments, while Ser-392 lies exactly 5 amino acids outside the C-terminus of the large α-helical domain. The homology between these two sites and their symmetry about the α helix suggested that Ser-22 and Ser-392 might be involved in the phosphorylation events affecting the assembly properties of the lamins. The demonstration by Ward and Kirschner (1990) that Ser-392 is specifically phosphorylated in response to MPF/*cdc2* and that Ser-22 is phosphorylated in both mitosis and interphase provided the impetus for a more detailed mutational analysis of these sites.

Phenotypes of Cells Transfected with Single Ser-392 and Ser-22 Mutants

To determine the effect of substitutions at Ser-22 or Ser-392 on nuclear events during the cell cycle, we constructed a series of mutants of the human lamin A cDNA and transfected them into CHO cells. Cells transiently expressing these constructs were detected using a mouse monoclonal antibody to the A and C lamins that recognizes the transfected human but not the endogenous CHO lamins (Loewinger and McKeon, 1988; Holtz et al., 1989). We have previously shown that human lamin A expressed in CHO cells behaves in a manner indistinguishable from that of the CHO lamins during all stages of the cell cycle, including the events of disassembly in mitosis and reassembly in telophase. This study essentially asks whether dominant-negative phenotypes (Herskowitz, 1987) affecting nuclear envelope disassembly result from mutations that eliminate the phosphorylation sites on the lamin A protein. A prerequisite for obtaining such phenotypes is a high level of expression of the transfected lamin A cDNA, because human lamin A is incorporated into the nuclear lamina together with the endogenous A, B, and C lamin proteins. Since the endogenous lamins would presumably be phosphorylated and disassembled in mitosis, the mutant proteins would have to form a concatenated

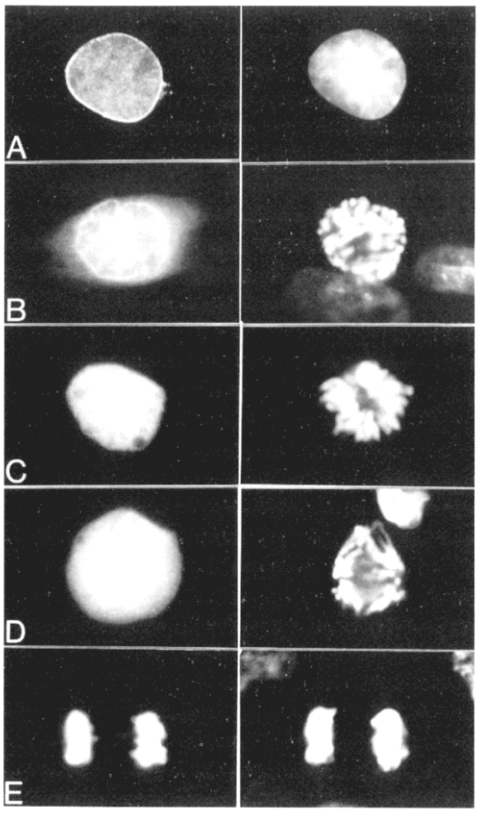

Figure 2. Wild-Type Phenotype of CHO Cells Transfected with Human Lamin A

The wild-type human lamin A cDNA was transfected into CHO cells and detected using a human-specific lamin monoclonal antibody (left). DNA was detected using Hoechst dye 33258 (right). (A) Interphase cell revealing an intact nuclear lamina. (B) Prophase cell in the process of solubilizing the nuclear lamina, which appears as soluble staining in the cytoplasm. The chromosomes are in an early stage of condensation. (C) Metaphase cell displaying completely diffuse lamin staining. CHO cells are highly rounded during mitosis. Chromosomes are fully condensed and aligned on a mitotic spindle. (D) Anaphase cell showing diffuse lamin staining and segregating chromosomes. (E) Telophase cell with lamins appearing on the decondensing chromosomes. This phenotype is also exhibited by cells transfected with the Ser-392→Ile mutant cDNA.

Table 1. Distribution of Mitotic Phenotypes

Transfected cDNA	Wild-Type Prophase	Mutant Prophase	Wild-Type Metaphase	Mutant Metaphase	Mutant Collapsed	Wild-Type Anaphase/ Telophase	Mutant Anaphase/ Telophase	Total Mutants
Wild type	15% (69)	1% (4)	15% (71)	0% (0)	0% (0)	69% (328)	1% (1)	2%
S-392→I	10% (54)	1% (3)	16% (81)	1% (1)	1% (5)	72% (369)	1% (2)	4%
S-22→A	15% (48)	11% (35)	17% (56)	6% (21)	8% (27)	58% (191)	10% (33)	35%
S-22→A/S-392→I	8% (61)	16% (56)	2% (8)	13% (45)	12% (42)	18% (61)	22% (75)	73%
S-22→A/S-392→N	13% (25)	15% (28)	3% (5)	13% (24)	9% (17)	28% (53)	19% (35)	56%
S-22→P/S-392→I	7% (15)	29% (66)	3% (6)	25% (56)	8% (19)	13% (30)	15% (35)	77%
S-22→A/S-390→E	25% (45)	6% (11)	10% (19)	7% (12)	1% (2)	40% (72)	13% (23)	27%
del($PS^{392}P$)	12% (43)	3% (12)	16% (61)	1% (5)	2% (8)	61% (226)	4% (14)	10%
del($PLS^{22}P$)	13% (28)	13% (30)	6% (13)	9% (20)	9% (21)	36% (81)	13% (30)	44%
del($PLS^{22}P$)/($PS^{392}P$)	22% (52)	28% (67)	0% (0)	14% (33)	30% (71)	4% (9)	3% (6)	75%

The mitotic phenotypes of individual transfected cells in this study were scored as one of seven categories judged by the state of nuclear lamina disassembly and chromosome condensation. The nuclear lamina was detected by indirect immunofluorescence using the human lamin A/C-specific monoclonal antibody and the state of chromosome condensation by the fluorescent DNA dye Hoechst 33258. The percentage of each phenotype is given for each construct, with the actual number in parentheses. (Column 2) Wild-type prophase cells were defined as those cells displaying a continuous nuclear lamina around condensed chromosomes located at the periphery of the nucleus. Cells in later stages of prophase, in which chromosomes are located away from the nuclear periphery, were also considered in this class if their nuclear laminae were thin and the cytoplasm showed some dispersed lamin staining (Figure 2B). (Column 3) Mutant prophase cells had a late prophase chromosome configuration, but an intact nuclear lamina. (Column 4) Wild-type metaphase cells had an aligned array of chromosomes and a dispersed distribution of nuclear lamins (Figure 2C). (Column 5) Mutant metaphase cells displayed an aligned array of chromosomes within an apparently continuous nuclear lamina (Figure 4D). (Column 6) The "collapsed" phenotype was marked by small or distorted nuclei having condensed chromosomes surrounded by an intact nuclear lamina. The lamina also typically possessed a corrugated appearance (Figure 5E). (Column 7) Wild-type anaphase and early telophase cells were grouped into a single category (Figure 2D and 2E). (Column 8) Mutant anaphase and telophase cells showed the anaphase and telophase chromosomes enclosed within a single lamina (Figures 4E and 4F). (Column 9) Total percentage of mutant mitotic cells for each construct.

network to resist disassembly together with the endogenous lamins. Because of the human specificity of the monoclonal antibody 1E4, we could not assay the state of the endogenous lamins in this study. Another limitation of this transient transfection system was that we could neither control nor ascertain the absolute levels of mutant lamin expression in any given cell. However, stable cell lines expressed wild-type human lamin A at levels similar in magnitude to those of the endogenous lamin proteins (Loewinger and McKeon, 1988).

Transfection of lamin A cDNAs harboring point mutations at Ser-392 (to Asn or Ile) had no effect on either the distribution or the behavior of the mutant protein during the cell cycle (Figure 2 and Table 1). The transfected cells were normal in morphology and proceeded through the usual stages of mitosis. This wild-type phenotype displays a well-defined nuclear envelope during interphase (Figure 2A), the beginning of lamin disassembly in prophase (Figure 2B), complete lamin disassembly in metaphase and anaphase (Figures 2C and 2D), and lamin reassembly in telophase (Figure 2E). Occasionally a "partial" phenotype was observed in cells transfected with these lamin A mutants, in which the nuclear lamina of metaphase or anaphase cells appeared partially undissolved. However, this effect was not dominant; transfected cells were capable of proceeding through mitosis (Figure 2 and Table 1).

Transfection of the lamin A cDNA bearing point mutations at Ser-22 resulted in unusual mitotic phenotypes marked by the persistence of the nuclear lamina. Approximately 35% of the transfected mitotic cells displayed an intact nuclear lamina at stages of chromosome condensation judged to be characteristic of late prophase, metaphase, or anaphase. We assigned four categories to the overall phenotype based on the state of chromosome condensation and the position of the chromosomes in the nucleus. The first mutant category was assigned to what appeared to be late prophase, in which the chromosomes no longer line the nuclear envelope but the transfected lamin A is still fully assembled at the nuclear periphery (Figure 3B). The second mutant category was interpreted to be metaphase because the chromosomes are ordered in a characteristic array, but again the transfected lamin A remains assembled at the nuclear periphery (Figure 3C). The third category was more difficult to interpret because the overall state of chromosome condensation and nuclear shape was unlike anything seen in cells transfected with the wild-type cDNA. These cells generally display smaller, elongated nuclei in which the chromosomes appear packed and distorted by the intact lamina (Figure 3D). This stage represented a relatively minor component (8%) of the mitotic profile (Table 1). The fourth mutant category was assigned to anaphase or telophase cells in which the daughter chromosomes or nuclei are surrounded by a single, continuous nuclear lamina (Figure 3E). This category constituted 10% of the total mitotic cells.

Apparent from the tabulations of the Ser-22→Ala transfections is that, although this mutant cDNA yields unusual phenotypes, the overall percentage of mitotic cells displaying an intact nuclear lamina was only 35% (Table 1). In particular, only 21 of 77 metaphase cells exhibited an intact lamina. Furthermore, many of the persistent nuclear laminae had small discontinuities, suggesting that partial disassembly had occurred (Figure 3). The "weakness" of the Ser-22→Ala mutant might be attributed to insufficient levels of expression, which would preclude the formation of an interconnected network of mutant lamin proteins.

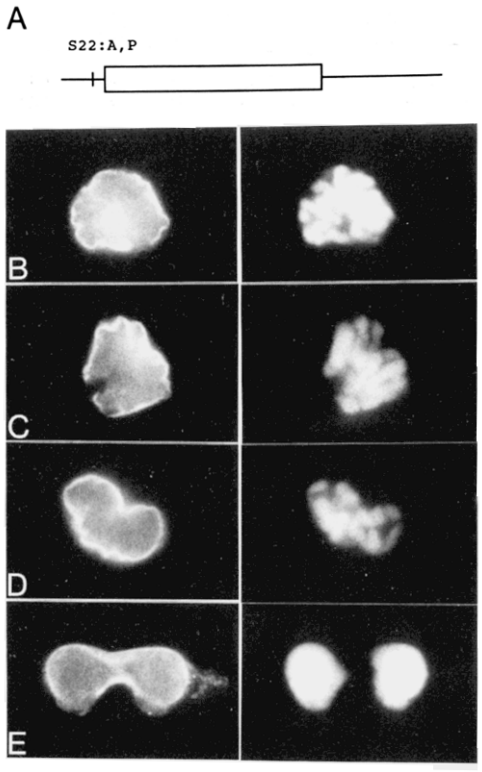

Figure 3. Phenotype of Cells Transfected with Single Ser-22→Ala Mutants

Expression of the Ser-22→Ala cDNA resulted in the abnormal persistence of a nuclear lamina in 35% of the mitotic cells. The schematic lamin A diagram in (A) shows the position of the point mutations. The four major stages of abnormal mitotic cells are pictured: (B) late prophase cell with an intact nuclear lamina, (C) metaphase cell enclosed within a nuclear lamina, (D) a collapsed nucleus containing condensed chromosomes, and (E) two daughter sets of chromosomes within a single lamina. (Left) Anti-human lamin staining. (Right) Hoechst dye (DNA) staining.

However, the finding that Ser-392 was the only new site of phosphorylation on lamin C in response to MPF/*cdc2* (Ward and Kirschner, 1990) suggested that, despite the wild-type appearance of cells transfected with the Ser-392 point mutant cDNAs, Ser-392 plays a coordinate role in lamina disassembly. We tested this possibility by constructing cDNAs with mutations that altered both Ser-22 and Ser-392.

Mitotic Phenotypes of Cells Transfected with Double Ser-22/Ser-392 Point Mutants

The transfection of double Ser-22/Ser-392 mutant cDNAs into CHO cells yielded the same phenotypes as the Ser-22 point mutant cDNAs, but the overall proportion of mitotic cells showing an intact nuclear lamina was much higher (35% for Ser-22→Ala versus 63% for Ser-22→Ala/Ser-392→Ile; Table 1). In addition, whereas only 27% of the metaphase cells expressing the Ser-22→Ala mutant displayed an intact nuclear lamina, 85% of those transfected with the Ser-22→Ala/Ser-392→Ile double mutant showed an intact lamina (Table 1). Because of this high percentage of phenotypic expression, we were able to reconstruct the progression of the Ser-22/Ser-392 double mutants through the mitotic cycle (Figure 4). The interphase transfected cells show a wild-type distribution of human lamin A at the nuclear envelope (Figure 4B), but the mutant protein appears more distinct than wild type (Figure 2A). Cells that have entered the mitotic cycle as indicated by chromosome condensation have the curious ability to continue though the cycle despite the apparently intact nuclear lamina. This progression is illustrated by the prophase cell (Figure 4C), the metaphase cell (Figure 4D), and the anaphase and telophase configurations (Figures 4E and 4F). If this interpretation is correct, it follows that chromosome segregation is unaffected by the presence of a nuclear lamina composed of the double Ser-22/Ser-392 mutant lamin A. Thus, while transfection of the double

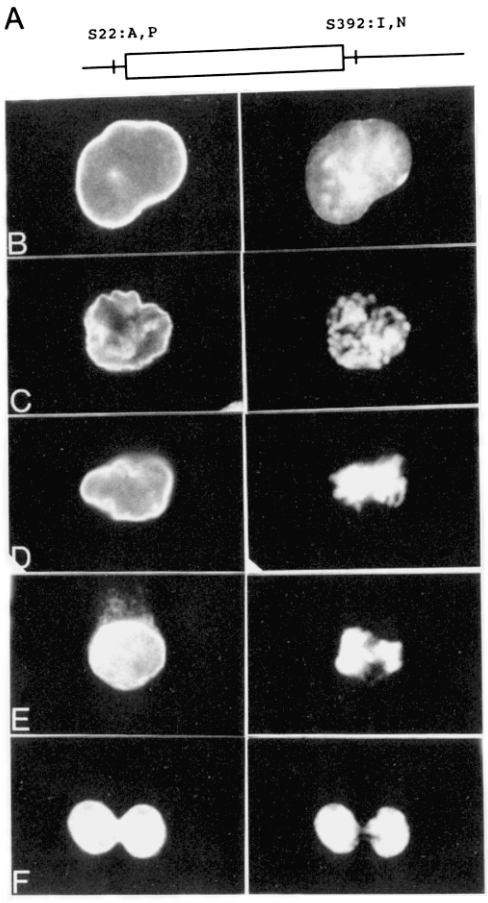

Figure 4. Phenotype of Cells Transfected with Double Ser-22/Ser-392 Point Mutants

Point mutations converting Ser-22 to Ala or Pro were introduced into cDNAs bearing Ser-392 mutations (to Ile or Asn) by using an intervening ApaI site, and the double mutants were expressed in CHO cells. (A) Schematic lamin A diagram showing the positions of the point mutations. (Left) Anti-human lamin staining. (Right) Hoechst dye (DNA) staining. (B) Interphase cell showing distinct nuclear lamina staining. (C) Prophase cell. (D) Metaphase cell, as judged by condensed chromosomes in a central position. (E) Anaphase cell (defined by separate groups of chromosomes) displaying a continuous nuclear lamina. (F) Telophase cell with an intact nuclear lamina but separate clusters of decondensing chromosomes.

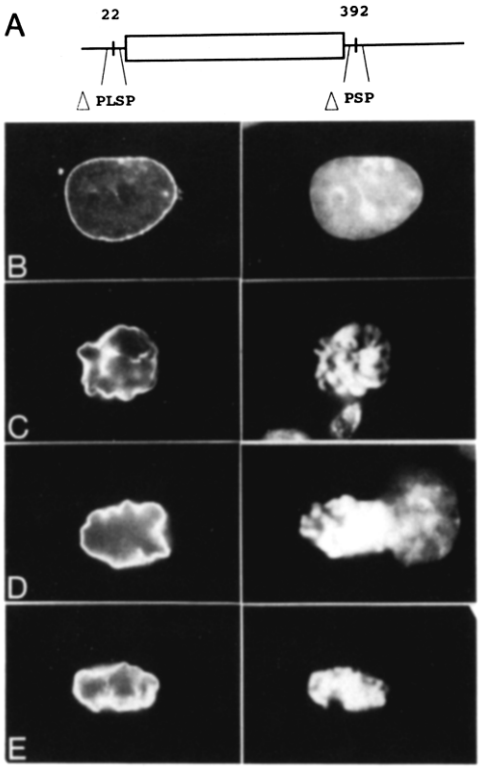

Figure 5. Mitotic Arrest of Cells Transfected with Double PLS^{22}P/PS^{392}P Deletion Mutants

Transfection of pHLA-del(PLS^{22}P)/(PS^{392}P) yields a population of cells essentially devoid of anaphase and telophase stages. (A) Schematic lamin A diagram showing the positions of the deletions. (B) Interphase cells with a distinct nuclear lamina. (C) Late prophase cell showing an intact lamina. (D and E) Metaphase cells with condensed chromosomes and a collapsed or deformed nuclear lamina. No evidence for chromosome segregation is apparent.

Ser-22/Ser-392 mutants yields a much higher percentage of mutant phenotypes than the single Ser-22 mutants, the stable nuclear lamina formed is apparently ineffective in preventing the invasion of spindle microtubules thought to underlie chromosome segregation (Mitchison, 1988).

To verify the contribution of the Ser-392 mutation to the high percentage of double mutant phenotypes, an additional double mutant was constructed in which the Ser-22 mutation was combined with a mutation at Ser-390. Upon transfection with the Ser-22→Ala/Ser-390→Glu mutant, 27% of the mitotic cells exhibited an intact nuclear envelope, a value more similar to that of single Ser-22 mutants (35%) than to the double mutant phenotype (56%–73%; Table 1). Thus the enhanced phenotypic effect of the Ser-392 mutation cannot be reproduced by a mutation at Ser-390.

A Double PLS^{22}P/PS^{392}P Deletion Results in Mitotic Arrest

The positioning of both Ser-22 and Ser-392 between two prolines suggested a possible role for these prolines in any phosphate-induced conformational change (such as proline isomerization; Evans et al., 1987; Lang et al., 1987). With this consideration, additional double mutants were constructed that lacked these sites along with their surrounding prolines. CHO cells transfected with pHLA-del(PLS^{22}P)/(PS^{392}P) (Figure 5A) displayed many of the same phenotypes seen with the double serine point mutants, including a wild-type interphase distribution (Figure 5B) and an intact lamin A network in both prophase and metaphase (Figures 5C and 5D). The overall mutant phenotype frequency was similar between the two types of double mutants. Double point mutations yielded between 56% and 77% mutant mitotic cells, while the double deletion mutations converted 75% of the mitotic cells to mutant phenotypes (Table 1). Notably, 100% of the metaphase cells expressing the double PLS^{22}P/PS^{392}P deletions displayed an intact nuclear envelope. Another interesting effect of the double deletion mutants was the near absence of anaphase or telophase cells. Instead, the distinctly different phenotype consisting of a collapsed network of lamin A surrounding condensed chromosomes predominates (Figure 5E). The chromosomes within these deformed networks of lamins are never in two polarized sets and therefore are not in anaphase. Often these chromosomes appear to be less condensed than wild type. The high frequency (30%) of this particular phenotype among the mitotic cells transfected with pHLA-del(PLS^{22}P/PS^{392}P)indicates that the cells are blocked before they enter anaphase (see Table 1). The 75% overall frequency of mutant phenotypes resulting from the double PLS^{22}P/PS^{392}P deletion also contrasts with the overall yield of mutant phenotypes from the single PLS^{22}P and PS^{392}P deletions, which gave 44% and 10% yields, respectively.

Mutations in the Terminal α-Helical Domains Prevent Assembly

The first 33 and the last 32 residues of the large α helix of the lamin proteins are highly conserved in all intermediate filament proteins (Geisler and Weber, 1982; McKeon et al., 1986). Although the function of these conserved end domains is not known, the α helix itself is centrally involved in the coiled-coil dimerization required for higher order assembly into 10 nm filaments. The close proximity and symmetry of Ser-22 and Ser-392 about these conserved blocks (Figure 1) prompted experiments to determine the sensitivity of these blocks to single point mutations. Figure 6 shows the schematized location of these sequences and an expanded version to identify precisely the target residue and assembly phenotype of the point mutants (A = assembly positive; N = assembly negative). Figures 6A and 6B show examples of wild-type assembly and the dispersed appearance of an assembly-negative phenotype. Evident from Figure 6 is that the point mutations in the non-α-helical regions had no effect on the assembly of these proteins, whereas many of the single changes within the conserved blocks resulted in assembly-negative phenotypes. Equally important is the observation that the point mutations placed in the α helix between the conserved end domains did not inhibit the assembly of the mutant lamin protein (Table 2). The heptad repeat pattern of the α-helical domain in the lamin pro-

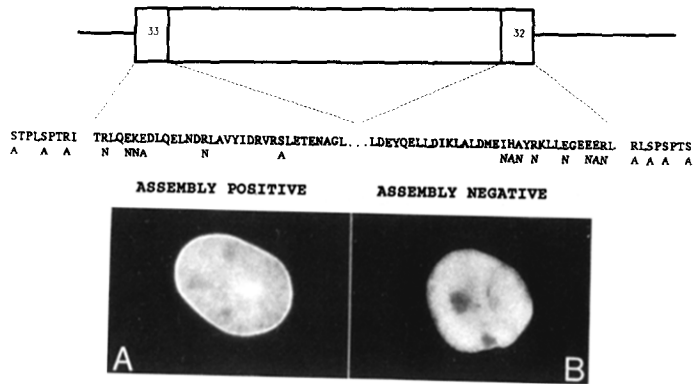

Figure 6. Effect of Mutations in the α-Helical End Domains on Assembly

Point mutations in the first 33 or the last 32 amino acids of the α helix were assayed for assembly capability. (A) Assembly-positive phenotype defined by a distinct lamina. (B) Assembly-negative phenotype marked by diffuse nuclear staining. A schematic diagram of the α helix and an expanded region of sequence is presented. Beneath the sequence is either an A, indicating the assembly-positive phenotype, or an N, for an assembly-negative phenotype for each point mutation. The changes introduced to amino acids outside the α helix had no obvious effect on assembly properties, while many of those within the conserved end domains of the α helix blocked assembly. Those which failed to block assembly occupied B, C, or F positions in the heptads, and thus lie on the surface of the dimer subunits (see Table 2 for details).

Table 2. Effects of Point Mutations on Assembly Properties

Residue	Change	Assembly	Position
Amino Terminus outside Helix			
Ser-18	Glu	+	–
Ser-22	Ala	+	–
Ser-22	Thr	+	–
Ser-22	Pro	+	–
Ser-22	Glu	+	–
Arg-25	Leu	+	–
Arg-25	His	+	–
Amino Terminus within Helix (Conserved Region)			
Arg-28	Thr	–	A
lys-32	Gln	–	E
Glu-33	Lys	+	F
Arg-41	His	–	G
Ser-51	Glu	+	C
Carboxyl Terminus within Helix (Nonconserved Region)			
Lys-341	Val	+	D
Arg-349	Val	+	E
Carboxyl Terminus within Helix (Conserved Region)			
Ile-373	Glu	–	A
His-374	Asn	+	B
Ala-375	Asp	–	C
Arg-377	His	–	E
Arg-377	Pro	–	E
Glu-381	Lys	–	B
Glu-384	Lys	–	E
Glu-385	Lys	+	F
Arg-386	Val	–	G
Arg-386	Leu	–	G
Arg-386	Pro	–	G
Carboxyl Terminus outside Helix			
Arg-388	Leu	+	–
Ser-390	Glu	+	–
Ser-392	Ile	+	–
Ser-392	Asn	+	–
Ser-395	Glu	+	–
Ser-404	Glu	+	–

Positions and changes of point mutations and their effect on the assembly potential of the expressed protein in interphase cells. Within the α-helical regions, specific heptad positions (A,B,C,D,E,F,G) are denoted. "+" = assembly positive; "–" = assembly negative.

tein predicts the surface positions of the amino acid residues of the coiled coil (McLachlan and Stewart, 1975; McLachlan, 1978). The A, D, E, and G positions denote amino acids facing the partner monomer of the unit dimer, on the inner surfaces of the coiled coil. The B, C, and F positions face outside the dimer and are thought to be important for higher order interactions with the surfaces of other dimers. Assembly-inhibiting point mutations in the α helix occurred at all A, D, E, and G positions tested, while most changes at residues pointing out of the dimer did not interrupt assembly (Table 2). The assembly-negative mutants remained diffuse throughout the cell cycle (data not shown).

Discussion

We have altered the amino acid sequences of two phosphorylation sites of lamin A and shown that expression of the mutant protein in cells blocks nuclear lamina disassembly in mitosis. These mutations affect two highly conserved serine residues that are symmetrically arranged 5 amino acids outside opposite ends of the large, 360 amino acid α helix required for higher order lamin assembly (Crick, 1953; McLachlan and Stewart, 1975; Albers and Fuchs, 1987; Loewinger and McKeon, 1988). In addition to their symmetry about the α helix, Ser-22 and Ser-392 exist in similar domains with the consensus sequence T/SP#SPT/S (# = single or no residue). These two serines have been shown to be phosphorylated in response to MPF/*cdc2* in mitosis, and Ser-392 in particular is only phosphorylated during mitosis (Ward and Kirschner, 1990). These data suggest a model for phosphorylation-induced plasticity and disassembly of the lamin proteins during the cell cycle and indirectly signify the importance of discrete regions of the α-helical domain for assembly.

Mutations Preventing Nuclear Lamina Disassembly

If the phosphorylation of Ser-22 and Ser-392 participates in the active disassembly of higher order lamin associations, we reasoned that mutations at either Ser-22 or Ser-392 would interfere with the disassembly process of these

mutant proteins in mitosis. Initially, Ser-392 was targeted for substitutions because this site is phosphorylated specifically in mitosis (Ward and Kirschner, 1990). We were dismayed to find no effect on the mitotic behavior of mutants in which Ser-392 was replaced by Ile or Asn. Subsequently, Ser-22, which is phosphorylated in interphase and hyperphosphorylated in mitosis, was substituted with Ala or Pro. Expression of these mutants resulted in a mitotic phenotype marked by the persistence of the nuclear lamina in approximately 35% of the mitotic cells (Table 1). Four categories of cells displaying an aberrantly intact nuclear lamina were recognized: late prophase cells with chromosomes away from the nuclear envelope (Figure 3B), metaphase cells with oriented chromosomes (Figure 3C), cells with a collapsed or distorted nuclear lamina surrounding tightly packed chromosomes (Figure 3D), and anaphase or early telophase cells with sets of chromosomes within a common lamina (Figure 3E).

A disturbing effect of the Ser-22 mutants is that the majority of transfected cells succeed in disassembling the mutant lamina in mitosis. In some cells that possess a mutant phenotype, the persistent nuclear lamina shows discontinuous regions, suggesting partial disassembly (Figure 3). While this could be explained by limitations of the transfection system (for example, insufficient levels of expression), another possibility is that Ser-392 plays a subtle role in lamin dynamics. Because of the symmetry of Ser-392 and Ser-22 with respect to the α helix and the finding of mitotic phosphorylation of Ser-392, double mutations altering both Ser-392 and Ser-22 were assayed for their ability to block nuclear lamina disassembly. Double point mutants induced strikingly higher overall levels of mitotic phenotypes (56%–77%) in comparison with the single Ser-22 mutants (35%). If metaphase cells, the most easily scored mutant category, are considered, the double Ser-22/Ser-392 mutants yield 82%–92% with an intact nuclear lamina, whereas expression of the Ser-22 mutant results in only a 27% mutant phenotype (Table 1). The enhancing effect of Ser-392 substitutions on the interference of Ser-22 mutations with nuclear lamina disassembly is difficult to explain in light of the wild-type phenotype created by single Ser-392 mutations. As a control, a substitution of Ser-390 was also combined with Ser-22→Ala and assayed for its effect. Ser-390→Glu as a single mutation has no effect (data not shown). The Ser-22→Ala/Ser-390→Glu double mutant induced an overall level of mitotic phenotypes (27%) similar to that of single Ser-22 point mutants (35%).

A characteristic of the phenotypes resulting from Ser-22 or double Ser-22/Ser-392 mutations is that chromosome condensation and even chromosome segregation appear to proceed (Figure 4). Although the independence of lamin disassembly and chromosome condensation has been well established (Newport and Spann, 1987), it was surprising that chromosome segregation, presumably dependent on spindle microtubules, occurred despite the presence of an apparently intact nuclear lamina. The effects of Ser-22 and Ser-22/Ser-392 mutations appear to be limited to the nuclear lamina and do not confer a mitotic cycle arrest, as stages characteristic of anaphase and telophase were apparent (Figure 3E and Figures 4E and 4F). In this situation, completion of nuclear lamina breakdown is not required for progression through mitosis. This contrasts with the progression requirement for completion of DNA replication or the successful assembly of the mitotic spindle (Murray and Kirschner, 1989). We are currently investigating spindle formation and microtubule interaction with the mutant nuclear lamina in transfected cells.

The phenotype associated with the Ser-22 and Ser-22/Ser-392 double point mutants, together with the positioning of Ser-22 and Ser-392 between two conserved proline residues (Figure 1), suggested that these prolines might play some role in the effect of phosphorylation on lamin dynamics. Therefore, double mutants lacking $PLS^{22}P$ and $PS^{392}P$ were constructed and transfected into CHO cells. The resulting phenotype was more severe than with the Ser-22/Ser-392 double point mutants. The cells were arrested in mitosis with no evidence of chromosome segregation or the stages of anaphase or telophase (Figure 5 and Table 1). Metaphase cells with dispersed lamins were not observed, and only 7% of the cells advanced to any stage of anaphase or telophase, compared with 28%–47% for the cells transfected with the double Ser-22/Ser-392 point mutants. The unusual "collapsed" category (Figure 5E) of mutant phenotypes accounted for fully 30% of the mitotic cells. One explanation for the increased severity of this phenotype is that double $PLS^{22}P$/$PS^{392}P$ deletions result in increased lamina stability in mitosis, which completely prevents the intrusion of spindle microtubules and consequently blocks the advance through mitosis. The more severe phenotype induced by the double $PLS^{22}P/PS^{392}P$ mutants might indicate that the major effects are not directly mediated by the placement of negative charge but rather through conformational changes as a consequence of the surrounding prolines. Proline isomerization is known to be important in protein folding (Evans et al., 1987; Lang et al., 1987). Certainly other explanations exist for the severe phenotype of the cells transfected with double $PLS^{22}P/PS^{392}P$ deletion mutants besides proline *cis-trans* isomerization, but definitive descriptions must await structural information.

The Conserved α-Helical End Domains Are Involved in Assembly

The symmetry of Ser-22 and Ser-392 about the N- and C-terminal domains of the α helix prompted a closer examination of the helix structure for clues on the effects of phosphorylation near the end domains. While the α helices are conserved at a secondary structural level in all intermediate filament proteins, only the first 33 and last 32 residues are conserved at the level of amino acids (Geisler and Weber, 1981, 1982). In human lamins A and C, these blocks include Thr-27 to Leu-59 and Leu-356 to Leu-387 (schematized in Figure 6). The function of these conserved end domains of the α helix is not known, but C-terminal deletions of as few as 5 amino acids compromise the assembly properties of the entire α helix of keratins as

Table 3. Sequences Homologous to the Ser-22 and Ser-392 Sites

Proteins	Ser-22	Ser-392
Lamin A (human)	QASS**TP**L**Ṡ**P**T**RITR	RLRL**SP**Ṡ**P**TSQRSR
PKC-γ (human)	PDSR**SP**I**SP**TPVPV	IPSP**SPSP**TDSKRC
Wee-1 (S. pombe)	SSTD**SP**P**SP**S**T**PSN	–
RNA polymerase II (mouse)	SPNY**TP**T**SP**S**S**YSPT (52 repeats)	–
Bicoid (Drosophila)	–	PNAL**TPSP**T**P**STPT
NF-1 (human)	DYYT**SP**S**SP**T**S**SSR	–
	GGAT**SP**T**SP**S**S**YSP	–
Oct-1	–	SPSL**SPSP**S**A**SAS**I**
cdc10 start (S. pombe)	–	NMQS**SPSP**S**S**SFLL
Per (Drosophila)	PASL**TP**T**SP**T**R**SPR	–
Rel	–	QQLY**SPSP**S**A**SSLL
Bcr (human)	–	SSRV**SPSP**T**T**YRMF

Amino acid sequences from the National Biomedical Research Foundation were scanned for the presence of the motif represented by six positions: 1 = S or T, 2 = P, 3 = X or none, 4 = S, 5 = P, and 6 = T or S. The output is aligned in two rows depending on whether the two prolines are separated by two amino acids, as with the site around Ser-22 (PLSP), or one, as with Ser-392 (PSP). Residues in the search motif are in boldface. PKC-γ: Coussens et al. (1986); Wee-1: Russell and Nurse (1987); RNA polymerase II: Cordon et al. (1985); Bicoid: Berleth et al. (1988); NF-1: Jones et al. (1987); Oct-1: Petryniak et al. (1990); Per: Reddy et al. (1986); Rel: Stephens et al. (1983), Wilhelmsen et al. (1984); Bcr: Hariharan and Adams (1987). Asterisks denote phosphorylated serines.

well as lamins (Albers and Fuchs, 1987; Loewinger and McKeon, 1988). Amino acids in these end domains were targeted for analysis by a number of point mutations to determine the sensitivity of assembly functions to perturbations. This analysis yielded two important results (Figure 6 and Table 2). The first was that most point mutations in these end domains completely disrupt assembly functions, while those in the non-α-helical regions or in the internal α-helical regions had no obvious effect. The second was that end domain amino acids that line the inner surface of the coiled-coil dimer (heptad positions A, D, E, and G) are more sensitive to changes than those on the surface of the dimer (heptad positions B, C, and F; Table 2). This observation was opposite to that which we had expected, because higher order assembly is considered to depend on the interactions of amino acids that lie between the dimers. Regardless, the assembly capabilities of lamin A can more easily be compromised by disturbances in internal dimerization sites than by disturbances of residues that point outward from the dimer. These findings suggest that relatively minor changes in the packing and structure of the end domains may translate into significant changes regulating higher order structure. The sensitivity of the end domains of the α helix to perturbations might explain, in part, the disassembly induced by the phosphorylation of Ser-22 and Ser-392.

The regulation of muscle glycogen phosphorylase by phosphorylation is understood at a structural level (Sprang et al., 1988). The key phosphorylation site on phosphorylase, Ser-14, is among a group of amino acids that has a random coil structure. As a consequence of phosphorylation, these N-terminal residues assume an ordered helix, which then interacts with the enzyme to stabilize its active conformation. In a possibly analogous manner, Ser-22 and Ser-392 of lamin A are in small domains predicted to have random structures immediately adjacent to the coiled-coil α helices (Chou and Fasman, 1978). The possibility exists that phosphorylation at Ser-22 and Ser-392 induces a more ordered conformation of these regions, the effects of which could be transmitted to the adjacent, hypersensitive α-helical end domains. The regulation of coiled-coil molecules by phosphorylation has a precedent in nonmuscle myosins. The C-terminus of Acanthamoeba myosin II contains an α helix of 663 amino acids terminated by a 29 amino acid, non-α-helical tail. The three phosphorylation sites that regulate myosin II ATPase activity lie within the short, non-α-helical tail (Cote et al., 1984). The mechanism by which these phosphorylation signals are transmitted to the ATPase domain, which lies at the other end of the large α helix, is not understood (Korn and Hammer, 1988), but might represent a problem analogous to that posed by the phosphorylation-induced lamin dynamics. Understanding the regulation of lamin assembly by phosphorylation will require more detailed structural information.

Several important biological and structural questions remain in understanding the coordinate interactions of cell cycle regulators with structural components of the nuclear lamina. The first is the identity of the kinase(s) that target the nuclear lamin proteins, their location in the cell, and their regulation by *cdc2*. *cdc2* has been identified as a gene encoding a protein kinase required for both the G1 to S and the G2 to M transitions in Schizosaccharomyces pombe (Nurse and Bissett, 1981). Although homologs have been identified in higher eukaryotes, the number and specificity of kinase complexes containing *cdc2* are not known (Lee and Nurse, 1987; McVey et al., 1989; Giordano et al., 1989).

The CTD kinase contains *cdc2* and phosphorylates target sites (C-terminal YSPTSPS repeats) on RNA polymerase II that are similar to the lamin Ser-22 and Ser-392 sites, S/TP#SPT/S. However, the CTD kinase presumably operates in interphase cells (Cordon et al., 1985; Cisek and Cordon, 1989). Mitotic phosphorylation sites on $pp60^{c\text{-}src}$ (consensus sequence: basic/polarS/TPXbasic) are thought to be the target of MPF/*cdc2* but have only weak homology to the lamin sites (Shenoy et al., 1989; Morgan et al., 1989). Probably the most unusual feature

Table 4. Mutagenic Oligonucleotides Used in Constructions

Mutant	Oligonucleotide
pHLA-S18:E	5′-CAG CGG AGT TTC GCT GGC CTG-3′
pHLA-S22:A	5′-GT GGG CGC CAG CGG ATG G-3′
pHLA-S22:T	T
phLA-S22:P	G
pHLA-S22:E	5′-AT GCG GGT GGG TTC CAG CGG AGT G-3′
pHLA-R25:L	5′-CCG GGT GAT GAG GGT GGG CGA-3′
pHLA-R25:H	T
PHLA-R28:T	5′-CTC CTG CAG CGT GGT GAT GCG-3′
pHLA-K32:Q	5′-CAG GTC CTC CTG CTC CTG CAG-3′
pHLA-E33:K	5′-CTG CAG GTC CTT CTT CTC CTG-3′
pHLA-R41:H	5′-GAC CGC CAA ATG ATC ATT GAG-3′
PHLA-K341:V	5′-TC CCG CTC TAC TTC CGC CA-3′
pHLA-R349:V	5′-AT CCT TGC TAC CAT CTC GG-3′
pHLA-I373:E	5′-GTA GGC GTG TTC CTC CAT GTC-3′
pHLA-H374:N	5′-GCG GTA GGC GTT GAT CTC CAT G-3′
pHLA-A375:D	5′-CTT GCG GTA ATC GTG GAT CTC-3′
pHLA-R377:H	5′-CAA GAG CTT GTG GTA GGC GTG-3′
pHLA-R377:P	G
pHLA-E381:K	5′-TC CTC GCC CTT CAA GAG CTT G-3′
pHLA-E384:K	5′-G TAG CCT CTC CTT CTC GCC CTC CA-3′
pHLA-E385:K	5′-GCG TAG CCT CTT CTC CTC GCC-3′
pHLA-R386:V	5′-CAG GCC TAG CAC CTC CTC CTC-3′
pHLA-R386:L	G
pHLA-R386:P	GG
pHLA-R388:L	5′-CT GGG GGA CAG GAG TAG CCT CTC-3′
pHLA-S390:E	5′-AGG GCT GGG TTC CAG GCG TAG-3′
pHLA-S392:I	5′-GA GGT AGG GAT GGG GGA C-3′
pHLA-S392:N	T
pHLA-S395:E	5′-GCT GCG CTG TTC GGT AGG GCT-3′
pHLA-S404:E	5′-GGA TGA GTG TTC GGA AGC ACG-3′

of all these sites is the presence of proline residues, which are not commonly found immediately adjacent to phosphorylated residues (Edelman et al., 1987; Vulliet et al., 1989). To identify other proteins bearing amino acid sequences similar to those of the lamin phosphorylation sites Ser-22 and Ser-392, we scanned protein data bases with the consensus sequence S/TP#SPT/S and aligned the output with either the Ser-22 or Ser-392 sites (Table 3). While a number of proteins possess the lamin S/TP# SPT/S sequence, in most cases specific regulatory phosphorylation sites of these proteins have not been identified. Of potential interest in light of the phosphorylation of the repeat motif of RNA polymerase II is the appearance of the S/TP#SPT/S sequences in domains thought to be required for transcriptional activation by Bicoid, CTF/NF-1, and Oct-1 (Struhl et al., 1989; Mermod et al., 1989; Petryniak et al., 1990).

Another important question concerns the individual contributions of the lamin A phosphorylation sites to the lamin dynamics in mitosis and interphase. Ser-22 and Ser-404 are phosphorylated in both interphase and mitosis (Ward and Kirschner, 1990). A role for Ser-404 in phosphorylation-induced lamin dynamics has not been identified, but like Ser-22, it may be important for maintaining the plasticity required for interphase nuclear envelope restructuring. While Ser-392, the only M phase–specific phosphorylation site, may play a disassembly-triggering role in mitosis, it is not absolutely required for lamin A disassembly in the transfection system used here because its substitution alone does not block disassembly in mitosis. Phosphorylation at Ser-392 might function within a cross–talk mechanism to influence the level of Ser-22 phosphorylation during the cell cycle.

One additional problem to assigning specific roles to the phosphorylation sites is that the in vivo stoichiometry of phosphorylation at any one site is not known. Consequently, the effects of coordinate increases or decreases of phosphorylation at these sites on lamin dynamics are uncertain. Although both the phosphorylation mapping data and the limited set of site-directed mutations point to a key role for Ser-932, a more complex series of double and triple mutants involving Ser-392, Ser-22, and Ser-404 are under construction to decipher the other necessary components of lamin dynamics. A molecular description of the effects of phosphorylation on lamin assembly remains to be illuminated: what is the structure of the apparently nonhelical regions surrounding Ser-22 and Ser-392 before phosphorylation and how do these sites change in response to phosphorylation? Structural analyses are underway to determine whether conformational changes are induced at Ser-22 and Ser-392 by cell cycle–regulated phosphorylation and, if so, how these changes are transmitted to the α-helical domain to affect higher order assembly.

Experimental Procedures

Oligonucleotide-Directed Mutagenesis

Plasmid Construction

Mutations were introduced into the coding region of the human lamin A cDNA using the double primer method (Zoller and Smith, 1984).

Single-stranded M13mp18 containing the wild-type lamin A cDNA was used as a template for second-strand synthesis, primed by mutant oligonucleotides and an M13 universal primer and using T4 polymerase. The mutagenic oligonucleotides employed and the plasmid designations are listed in Table 4.

Point mutations or deletions were detected by differential hybridization of ^{32}P-labeled mutant oligonucleotides to plaques lifted onto nitrocellulose from a lawn of JM101. Thermostable plaques were selected and purified phage sequenced using standard dideoxy chain termination methods (Ausubel et al., 1987). The desired mutant inserts were removed from RF mp18 DNA by digestion with EcoRI and XbaI and, after separation by low melting point gel electrophoresis, subcloned into the mammalian expression vector pECE (Ellis et al., 1986).

Double Mutant Constructions

Double mutations altering both the amino and carboxyl ends of the α helix were made using the intervening ApaI site (at amino acids 249–250) along with the XbaI site at the 3′ end of the cDNA. Fragments were separated on low melting point agarose gels and the desired pieces isolated and ligated into a single plasmid. Plasmids were propagated in XL-1 blue (Stratagene) and purified by alkaline–SDS lysis followed by two rounds of centrifugation in CsCl gradients.

DNA Transfections

CHO cells were grown in α-MEM media plus glutamine (Hazelton) supplemented with 15% fetal calf serum (Hyclone) in a 37°C, 5% CO_2 incubator. Cells were plated on 18 mm round coverslips at a concentration of approximately 1 × 10^5 cells per ml the day before transfecting. DNA (1–3 μg) was precipitated by the calcium phosphate method (Ausubel et al., 1987). Slowly and with stirring, 30 μl of 2× HEPES buffer saline (282 mM NaCl, 50 mM HEPES, 0.78 mM Na_2HPO_4 [pH 7.5]) was added to a mixture of the DNA plus 30 μl of 0.2 M $CaCl_2$. After a 20 min incubation at room temperature, 350 μl of complete media was added, and the mixture was placed on the coverslips for 4 hr in the incubator. At this time the cells were rinsed a few times and refed with complete media and allowed to incubate for another 12–16 hr at 37°C.

Immunofluorescence

Cells were fixed by treatment with 1% formaldehyde in PBS for 5 min, rinsed several times with PBS plus 0.1% NP40 (PBS-NP40), and incubated for 30 min at room temperature with a mouse monoclonal antibody against the human A and C lamins that does not recognize the endogenous CHO lamins (Loewinger and McKeon, 1988). After several rinses with PBS-NP40, a rhodamine-conjugated, goat anti-mouse secondary antibody (Boehringer Mannheim) was added for another 30 min incubation. The cells were also treated with the DNA stain bisbenzimide (Hoechst 33258) at 10 μg/ml for 1 min, before the coverslips were mounted in 90% glycerol and viewed with a Zeiss Axiophot fluorescence microscope.

Slides were scanned, and each transfected mitotic cell was classified as prophase, metaphase, anaphase, or telophase according to the state of chromosome condensation observed under Hoechst filters (Table 1). Before any transfection was scored, it was necessary to ascertain whether the wild-type protein derived from expression of pHLA was assembling at the nuclear envelope of interphase cells. This is important because over the past 18 months of this study, we have encountered three periods lasting 4 weeks to 2 months when the transfected human A lamin does not assemble, but rather remains diffuse in the nucleus. The key variable was determined to be the lot of fetal bovine serum. Thus it was important to test various lots for the ability of the transfected human A lamin to assemble at interphase nuclear envelopes.

Acknowledgments

We thank Gary Ward, Marc Kirschner, Brian Burke, Martyn Botfield, James Conway, and David Parry for helpful discussions throughout the course of this work. We are grateful to Temple Smith for performing the protein data base search. We thank Michael Isacco for inspiration and encouragement. This research was supported by grants from the National Institutes of Health, the National Health Research Foundation, and the Lucille P. Markey Charitable Trust.

The costs of publication of this article were defrayed in part by the payment of page charges. This article must therefore be hereby marked "*advertisement*" in accordance with 18 U.S.C. Section 1734 solely to indicate this fact.

Received December 20, 1989; revised February 23, 1990.

References

Aebi, U., Cohn, J. B., Buhle, L., and Gerace, L. (1986). The nuclear lamina is a meshwork of intermediate type filaments. Nature *323*, 560–564.

Albers, K., and Fuchs, E. (1987). The expression of mutant epidermal keratin cDNAs transfected in simple epithelial and squamous cell carcinoma lines. J. Cell Biol. *105*, 791–806.

Ausubel, F. M., Brent, R., Kingston, R. E., Moore, D. D., Smith, J. A., Seidman, J. G., and Struhl, K. (1987). Current Protocols in Molecular Biology (New York: John Wiley & Sons).

Berleth, T., Burri, M., Thoma, G., Bopp, D., Richstein, S., Frigerio, G., Noll, M., and Nusslein-Volhard, C. (1988). The role of localization of bicoid RNA in organizing the anterior pattern of the *Drosophila* embryo. EMBO J. *7*, 1749–1756.

Burke, B., and Gerace, L. (1986). A cell free system to study reassembly of the nuclear envelope at the end of mitosis. Cell *44*, 639–652.

Chou, P. Y., and Fasman, G. D. (1978). Production of the secondary structure of proteins from their amino acid sequence. Adv. Enzymol. *47*, 45–148.

Chou, Y. H., Rosevear, E., and Goldman, R. D. (1989). Phosphorylation and disassembly of intermediate filaments in mitotic cells. Proc. Natl. Acad. Sci. USA *86*, 1885–1889.

Cisek, L. J., and Cordon, J. L. (1989). Phosphorylation of RNA polymerase by a murine homologue of the cell-cycle control protein cdc2. Nature *339*, 679–684.

Cordon, J. L., Cadena, D. L., Ahearn, J. M., and Dahmus, M. E. (1985). A unique structure at the carboxyl terminus of the largest subunit of eukaryotic RNA polymerase II. Proc. Natl. Acad. Sci. USA *82*, 7934–7938.

Cote, G. P., Robinson, E. A., Appella, E., and Korn, E. D. (1984). Amino acid sequence of a segment of the *Acanthamoeba* myosin II heavy chain containing all three regulatory phosphorylation sites. J. Biol. Chem. *259*, 12781–12787.

Coussens, L., Parker, P. J., Rhee, L., Yang-Feng, T. L., Chen, E., Waterfield, M. D., Francke, U., and Ullrich, A. (1986). Multiple, distinct forms of bovine and human protein kinase C suggest diversity in cellular signaling pathways. Science *233*, 859–866.

Crick, F. H. C. (1953). The packing of alpha-helices: simple coiled-coils. Acta Cryst. *6*, 689–697.

Dessev, G., Iovcheva, C., Tasheva, B., and Goldman, R. (1988). Protein kinase activity associated with the nuclear envelope. Proc. Natl. Acad. Sci. USA *85*, 2994–2998.

Edelman, A. M., Blumenthal, D. K., and Krebs, E. G. (1987). Protein serine/threonine kinases. Annu. Rev. Biochem. *56*, 567–613.

Ellis, L., Clauser, E., Morgan, D. O., Edery, M., Roth, R. A., and Rutter, W. J. (1986). Replacement of insulin tyrosine residues 1162 and 1163 compromises insulin-stimulated kinase activity and uptake of 2-deoxyglucose. Cell *45*, 721–732.

Evans, P. A., Dobson, C. M., Kautz, R. A., Hatfull, G., and Fox, R. O. (1987). Proline isomerization in staphylococcal nuclear characterized by NMR and site-directed mutagenesis. Nature *329*, 266–270.

Fisher, D. Z., Chaudhary, N., and Blobel, G. (1986). cDNA sequencing of nuclear lamins A and C reveals primary and secondary structural homology to intermediate filaments. Proc. Natl. Acad. Sci. USA *83*, 6450–6454.

Franke, W. W., Schmid, E., Osborn, M., and Weber, K. (1978). Different intermediate-sized filaments distinguished by immunofluorescence microscopy. Proc. Natl. Acad. Sci. USA *75*, 5034–5038.

Geisler, N., and Weber, K. (1981). Comparison of the proteins of two immunologically distinct intermediate-sized filaments by amino-acid sequence analysis: desmin and vimentin. Proc. Natl. Acad. Sci. USA *78*, 4120–4123.

Geisler, N., and Weber, K. (1982). The amino acid sequence of chicken

muscle desmin provides a common structural model for intermediate filament proteins including the wool alpha keratins. EMBO J. *1*, 1649–1656.

Gerace, L., and Blobel, G. (1980). The nuclear envelope lamina is reversibly depolymerized during mitosis. Cell *19*, 277–287.

Gerace, L., and Burke, B. (1988). Functional organization of the nuclear envelope. Annu. Rev. Cell Biol. *4*, 335–374.

Giordano, A., Whyte, P., Harlow, E., Franza, B. R., Jr., Beach, D., and Draetta, G. (1989). A 60 kd cdc2-associated polypeptide complexes with the E1A proteins in adenovirus-infected cells. Cell *58*, 981–990.

Hariharan, I. K., and Adams, J. M. (1987). cDNA sequence for human *bcr*, the gene that translocates to the *abl* oncogene in chronic myeloid leukaemia. EMBO J. *6*, 115–119.

Herskowitz, I. (1987). Functional inactivation of genes by dominant negative mutations. Nature *329*, 219–222.

Hoger, T. H., Krohne, G., and Franke, W. (1988). Amino acid sequence and molecular characterization of murine lamin B as deduced from cDNA clones. Eur. J. Cell Biol. *47*, 283–290.

Holtz, D., Tanaka, R. A., Hartwig, J., and McKeon, F. (1989). The CaaX motif of lamin A functions in conjunction with the nuclear localization signal to target assembly to the nuclear envelope. Cell *59*, 969–977.

Hynes, R. O., and Destree, A. T. (1978). 10 nm filaments in normal and transformed cells. Cell *13*, 151–163.

Jones, K. A., Kadonaga, J. T., Rosenfeld, P. J., Kelly, T. J., and Tjian, R. (1987). A cellular DNA-binding protein that activates eukaryotic transcription and DNA replication. Cell *48*, 79–89.

Korn, E. D., and Hammer, J. A. (1988). Myosins of nonmuscle cells. Annu. Rev. Biophys. Chem. *17*, 23–45.

Krohne, G., Wolin, S. L., McKeon, F. D., Franke, W. W., and Kirschner, M. W. (1987). Nuclear lamin L_1 of *Xenopus laevis*: cDNA cloning, amino acid sequence and binding of a member of the lamin B subfamily. EMBO J. *6*, 3801–3808.

Lang, K., Schmid, F. X., and Fischer, G. (1987). Catalysis of protein folding by prolyl isomerase. Nature *329*, 268–270.

Lee, M. G., and Nurse, P. (1987). Complementation used to clone a human homologue of the fission yeast cell cycle control gene *cdc2*. Nature *327*, 31–35.

Loewinger, L., and McKeon, F. (1988). Mutations in the nuclear lamin proteins resulting in their aberrant assembly in the cytoplasm. EMBO J. *7*, 2301–2309.

Maller, J., Wu, M., and Gerhart, J. C. (1977). Changes in protein phosphorylation accompanying maturation of *Xenopus laevis* oocytes. Dev. Biol. *58*, 295–312.

McKeon, F. D., Kirschner, M. W., and Caput, D. (1986). Primary and secondary structural homology between the major nuclear envelope and cytoplasmic intermediate filament proteins. Nature *319*, 463–468.

McLachlan, A. D. (1978). Coiled-coil formation and sequence regularities in the helical regions of alpha-keratin. J. Mol. Biol. *124*, 293–304.

McLachlan, A. D., and Stewart, M. (1975). Tropomyosin coiled-coil interactions: evidence for an unstaggered structure. J. Mol. Biol. *98*, 293–304.

McVey, D., Brizuela, L., Mohr, I., Marshak, D. R., Gluzman, Y., and Beach, D. (1989). Phosphorylation of large tumor antigen by cdc2 stimulates SV40 DNA replication. Nature *341*, 503–507.

Mermod, N., O'Neill, E. A., Kelly, T. J., and Tjian, R. (1989). The proline-rich transcriptional activator of CTF/NF-1 is distinct from the replication and DNA binding domain. Cell *58*, 741–753.

Miake-Lye, R., and Kirschner, M. W. (1985). Induction of early mitotic events in a cell-free system. Cell *41*, 165–175.

Mitchison, T. J. (1988). Microtubule dynamics and kinetochore function in mitosis. Annu. Rev. Cell Biol. *4*, 527–549.

Morgan, D. O., Kaplan, J. M., Bishop, J. M., and Varmus, H. E. (1989). Mitosis-specific phosphorylation of $p60^{c\text{-}src}$ by $p34^{cdc2}$-associated protein kinase. Cell *57*, 775–786.

Murray, A. W., and Kirschner, M. W. (1989). Dominoes and clocks: the union of two views of the cell cycle. Science *246*, 614–621.

Newport, J. W., and Forbes, D. J. (1987). The nucleus: structure, function, and dynamics. Annu. Rev. Biochem. *56*, 535–565.

Newport, J., and Spann, T. (1987). Disassembly of the nucleus in mitotic extracts: membrane vesicularization, lamin disassembly, and chromosome condensation are independent processes. Cell *48*, 219–230.

Nurse, P., and Bissett, Y. (1981). Gene required in G1 for commitment to cell cycle and in G2 for control of mitosis in fission yeast. Nature *292*, 558–560.

Ottaviano, Y. L., and Gerace, L. (1985). Phosphorylation of the nuclear lamins during interphase and mitosis. J. Biol. Chem. *260*, 624–632.

Parry, D. A. D., Conway, J. F., Goldman, A. E., Goldman, R. D., and Steinert, P. M. (1987). Nuclear lamin proteins: common structures for paracrystalline, filamentous and lattice forms. Int. J. Biol. Macromol. *9*, 137–145.

Petryniak, B., Staudt, L. M., Postema, C. E., McCormack, W. T., and Thompson, C. B. (1990). Characterization of chicken octomer-binding proteins demonstrates that POU domain-containing homeobox transcription factors have been highly conserved during vertebrate evolution. Proc. Natl. Acad. Sci. USA *87*, 1099–1103.

Reddy, P., Jacquier, A. C., Abovich, N., Petersen, G., and Roshbash, M. (1986). The *period* clock locus of D. melanogaster codes for a proteoglycan. Cell *46*, 53–61.

Russell, P., and Nurse, P. (1987). Negative regulation of mitosis by *wee1+*, a gene encoding a protein kinase homolog. Cell *49*, 559–567.

Shenoy, S., Choi, J.-K., Bagrodia, S., Copeland, T. D., Maller, J. L., and Shalloway, D. (1989). Purified maturation promoting factor phosphorylates $pp60^{c\text{-}src}$ at the sites phosphorylated during fibroblast mitosis. Cell *57*, 763–774.

Sprang, S. R., Acharya, K. R., Goldsmith, E. J., Stuart, D. I., Varill, K., Fletterick, R. J., Madsen, N. B., and Johnson, L. N. (1988). Structural changes in glycogen phosphorylase induced by phosphorylation. Nature *336*, 215–221.

Stephens, R. M., Rice, N. R., Hiebsch, R. R., Bose, H. R., and Gilden, R. V. (1983). Nucleotide sequence of v-*rel*: the oncogene of reticuloendotheliosis virus. Proc. Natl. Acad. Sci. USA *80*, 6229–6233.

Struhl, G., Struhl, K., and Macdonald, P. M. (1989). The gradient morphogen *bicoid* is a concentration-dependent transcriptional activator. Cell *57*, 1259–1273.

Vulliet, P. R., Hall, F. L., Mitchell, J. P., and Hardie, D. G. (1989). Identification of a novel proline-directed serine/threonine protein kinase. J. Biol. Chem. *264*, 16292–16292.

Ward, G. E., and Kirschner, M. W. (1990). Identification of cell cycle-regulated phosphorylation sites on nuclear lamin C. Cell, this issue.

Wilhelmsen, K. C., Eggleton, K., and Temin, H. M. (1984). Nucleic acid sequences of the oncogene v-*rel* in reticuloendotheliosis virus strain T and its cellular homolog, the proto-oncogene c-*rel*. J. Virol. *52*, 172–182.

Wolin, S. L., Krohne, G., and Kirschner, M. W. (1987). A new lamin in *Xenopus* somatic tissues displays strong homology to human lamin A. EMBO J. *6*, 3809–3818.

Zoller, M. J., and Smith, M. (1984). Oligonucleotide-directed mutagenesis: a simple method using two oligonucleotide primers and a single-stranded DNA template. DNA *3*, 479–488.